357. Identification of motion parameters from images produced by atomic force microscopy

E. Sakyte[1], L. Saunoriene[1], M. Ragulskis[1], R. Maskeliunas[2]
[1]Kaunas University of Technology,
Studentu 50-222, LT-51368, Kaunas, Lithuania
[2]Vilnius Gediminas Technical University,
J. Basanaviciaus 28, Vilnius LT-03224, Lithuania
E-mail: [1] *edita.sakyte@ktu.lt* [1] *loreta.saunoriene@ktu.lt* [1] *minvydas.ragulskis@ktu.lt*
[2] *rimas.maskeliunas@me.vgtu.lt*

(Received 24 March 2008; accepted 13 June 2008)

Abstract. An experimental technique for analysis of pseudo-static oscillations of piezoelectric ceramics is presented in this paper. This technique is capable to detect both transverse and longitudinal oscillations and is based on the formation of observable grating modulated on the static surface of the scanned body. Mathematical and numerical models of the analyzed system comprising a scanning cantilever of atomic force microscope are presented in order to develop an experimental methodology to assess the frequency, transverse and longitudinal amplitudes of elliptic oscillations of the investigated systems.

Keywords: Atomic force microscopy, Digital image, Grating, Inverse problem.

Introduction

Sub-micrometer amplitude vibrations play an important role in different physical and engineering systems. Ultrasonic motors are typical examples of application of such vibrations. The vibration energy of piezoelectric ceramics is transferred to longitudinal or rotational motion of the elements of these motors [1-3].

Experimental measurement of transverse vibrations of piezoceramics excited by an oscillating charge is a complicated technical challenge first of all due to the fact that the amplitudes of these oscillations are small. The problem gets even harder when the frequency of excitation is far from the resonance frequencies of piezoelectric ceramics [4]. Pseudo static (low frequency) excitation produces even smaller deformations of the piezoelectric ceramics. Nevertheless, possibility of direct registration of transverse oscillations of electrically excited piezoceramics would be of great interest not only for the designers of ultrasonic motors [5], but also for many other different applications of piezoelectric materials [6].

Atomic force microscopy (AFM) is effectively applied for the measurement of nano-scale displacement, strain, thermal deformation fields [7-9]. This paper is focused on the applicability of AFM for the measurement of dynamic displacements of electrically excited piezoelectric ceramic materials even far away from their resonance frequencies.

Applicability of AFM techniques for measurement transverse vibrations of piezoelectric materials is analysed in [10]. The purpose of this paper is the development of techniques for analysis of general type response (not only transverse oscillations) of piezoelectric ceramics to electric excitation by means of atomic force microscopy. Interpretation of the experimental results provides insight into the physical processes taking place in the analysed objects.

Basic Numerical Model

Let's assume that a flat non-deformable surface is parallel to plane x–y and performs harmonic oscillations in the z-direction (Fig. 1). The amplitude of oscillations is A; angular frequency and phase – ω and φ. The maximum travel of the AFM scanner in the x-direction is L. It is assumed that the modulus of the scanner's travel velocity v

in the *x*-direction is constant, distance between the raster lines is *d*; scanning direction is reversed instantaneously.

The output of the measurement system is the instantaneous height of the scanned surface. It is clear that the elevation of the scanned surface will be falsely represented by height.

Let's assume that the scanner starts the scanning process at time moment t_0. Then the scanned instantaneous height at the right end of the first scanning line is $A\sin(\omega t_0 + \varphi)$. Time needed for the scanner to travel along the first scanning line is *L*/*v*. Thus, the scanned height at any *x* along the first scanning line (forth scan) is:

$$A\sin\left(\omega\left(t_0 + \frac{x}{v}\right) + \varphi\right) = A\sin\left(\frac{\omega}{v}x + \delta_0\right), \quad (1)$$

where $\delta_0 = \omega t_0 + \varphi$. Time needed to return to the beginning of the second scanning line from the end of the first scanning line is also *L*/*v*. Then, the scanned height along the second scanning line is:

$$A\sin\left(\frac{\omega}{v}x + \frac{2L\omega}{v} + \delta_0\right). \quad (2)$$

In other words, the graph of the harmonic function in the second scan (eq. (2)) is shifted to the left by phase $2L\omega v^{-1}$ with respect to the first scan (eq. (1)). Keeping in mind that the functions are harmonic (with period $\frac{2\pi v}{\omega}$), the observed shift is $\arg\left(2L\omega v^{-1}\right)$, here the function arg is defined as:

$$\arg(x) = x + k\cdot\frac{2\pi v}{\omega};\ k \in Z,\quad -\frac{\pi v}{\omega} < \arg(x) \le \frac{\pi v}{\omega}. \quad (3)$$

Then, the angle of the observed shift is (Fig. 2):

$$\alpha = \arctan\left(\arg\left(2L\omega v^{-1}\right)/d\right). \quad (4)$$

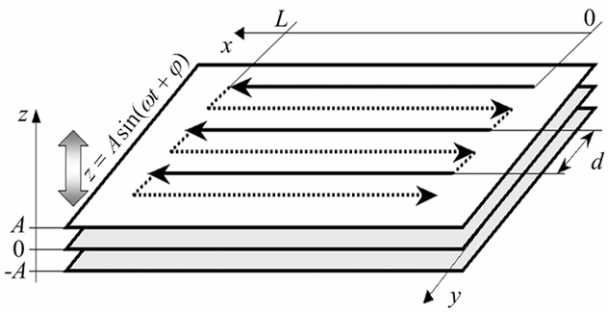

Fig. 1. Scan over an oscillating plate - a schematic diagram

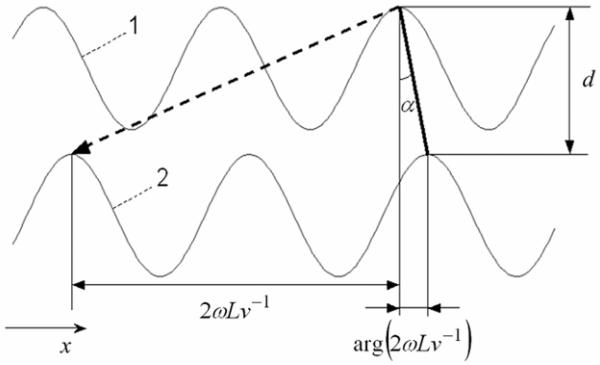

Fig. 2. The observed shift between scanning lines; 1 – the first line; 2 – the second line of the forth scan

If the scanning direction would be reversed, the total shift would be $-2L\omega v^{-1}$ and the angle of the observed shift would be

$$\alpha = \arctan\left(\arg\left(-2L\omega v^{-1}\right)/d\right). \quad (5)$$

Formation of observable grating caused by oscillation of a scanned surface can be effectively exploited for the identification of parameters of that oscillation. Identification of angular frequency of oscillation is straightforward and comprises two basic steps. First, the distance between the centres of grating lines λ must be measured along the scan direction. Then the angular frequency of oscillations can be determined from the following equation:

$$\omega = \frac{v}{\lambda}. \quad (6)$$

It can be noted that the basic numerical model evaluates only transverse oscillations of the plane *x*–*y* in the *z*-direction.

Experimental Investigations

The experimental set-up comprises an AFM, piezoelectric ceramics (5 mm × 10 mm × 3 mm) placed on the measurement table and a power amplifier producing oscillating charge. Two thin copper wires (0,05 mm diameter each) are welded to the side electrodes of the ceramics and connected to the power amplifier. The scanning area is set to 3,0 × 3,0 μm (the maximum travel of the scanner *L* = 3,0 μm). The sweep frequency is 1 Hz – the scanner sweeps over the scanning area forth and back in 1 s; scanning speed *v* = 6,0 μm/s. The produced digital image of the scanned area consists from 512 × 512 pixels (512 scan lines in forth or in back direction); *d* = 0,00625 μm. Time required to perform full surface scan is 512 s.

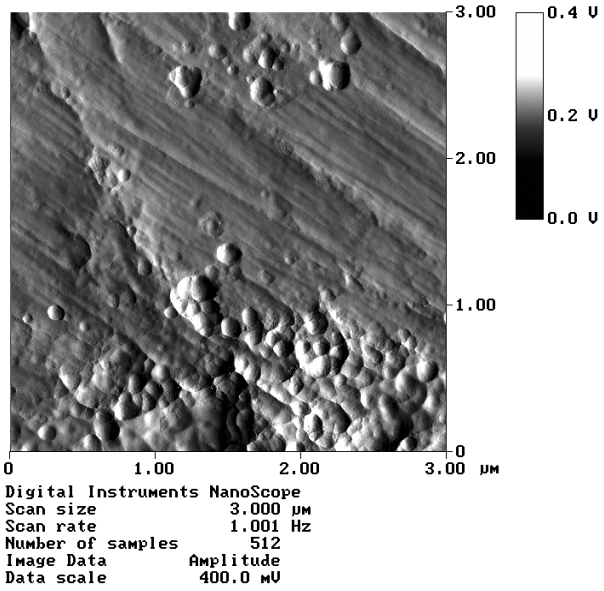

Fig. 3. AFM image of the static surface

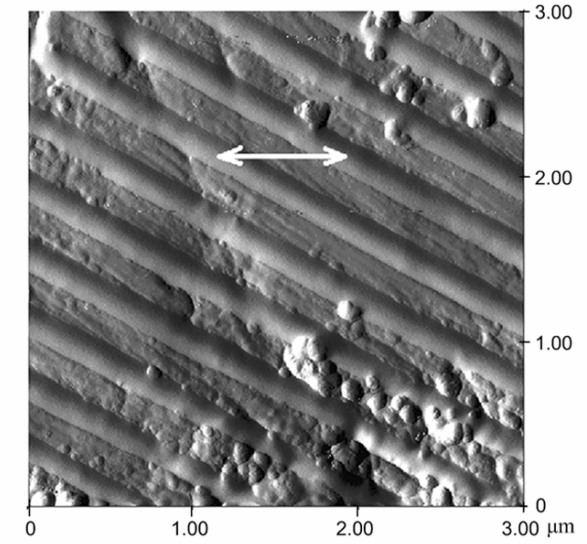

Fig. 4. Digital image of the scanned surface – 2D projection, forward scan

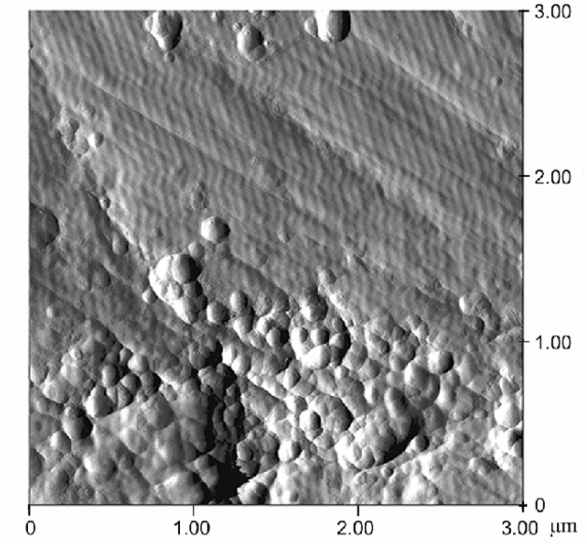

Fig. 5. Digital image of the scanned surface; ω = 100 Hz

AFM image of the static surface is presented in Fig. 3. The surface of piezoelectric ceramic was polished with fine grain abrasive paper – one can note definite oblique trenches produced during the process of finishing.

AFM images of the piezoelectric ceramics excited by oscillating charge are presented in Fig. 4. The angle of the observable grating produced by the periodic elevation of the surface and modulated on top of the static surface shows good agreement with equation (4). The white arrow in Fig. 4 shows the measured distance between the centres of grating lines (along the scan direction) what produces $\lambda = 0.817$. The reconstructed frequency is then $\omega = 7.34$ Hz, what is a perfect fit with the experimental setup.

If the excitation frequency is increased, the produced experimental AFM images still demonstrate the effect of observable grating (Fig. 5). Nevertheless, one can note that the grating lines are not straight. The following analysis tries to interpret and explain this effect which does not fit into the model described by equations eq. (1) – eq. (6).

Numerical Analysis

It is clear that though the frequency of excitation of piezoelectric ceramics is much lower that its resonant frequency, one cannot expect that the surface of ceramics will oscillate only in the transverse direction to the surface. The basic numerical model (Fig. 1) assumed ideally flat surface and any longitudinal motions of the surface would have no impact for the generated grating caused by elevation.

But our surface is not flat (Fig. 3). The image of the scanned surface will clearly be under the influence of any longitudinal motion of the surface. Therefore there exists a definite need for a numerical model explaining the observed effect of curvy grating modulated on top of the static surface (Fig. 5).

The numerical model of the scanning process is developed in Matlab environment. Initially it is assumed that the static surface has a shape as demonstrated in Fig. 6.

Assumption that the surface oscillates only in the transverse direction produces a clearly interpretable effect of observable grating. Pure longitudinal oscillations produce a fractures image of the surface without any observable grating. Elliptic motion of the surface produces both the interpretable grating and a fractured image of the surface (Fig. 7).

Detailed analysis of Fig. 7 and Fig. 8 reveals that the observable grating lines are straight what contradicts to the experimental results. On the contrary, analysis of the experimental image (Fig. 5) shows that the static image is not fractured.

The explanation comes from the inherent feature of experimental visualisation software used for the generation of digital images from AFM scans [8]. Two neighbouring scanning lines are automatically correlated for the local micro-surface properties. The calculated lag is used to shift the new scanning line in respect of the

previous scanning line in order to produce a smooth surface. What happens is that the reconstructed image of the surface becomes smooth, but the observable grating lines fractionise (Fig. 5).

Digital procedure of the correlation between two neighbouring scanning lines can be illustrated by the following one-dimensional example.

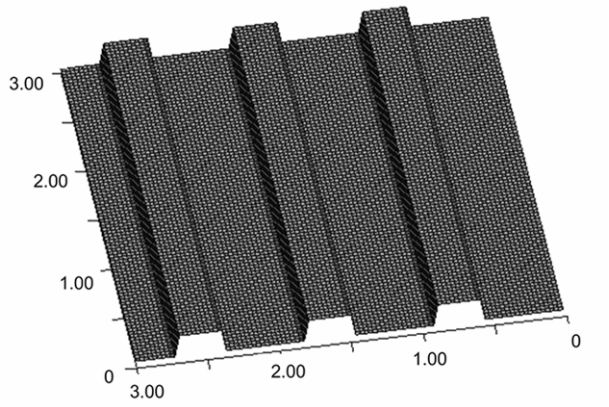

Fig. 6. Numerical model of a static surface

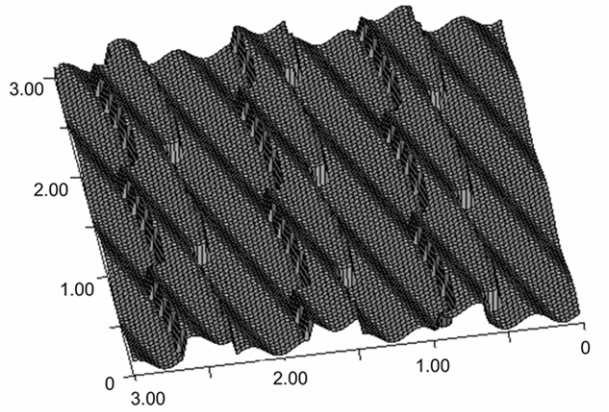

Fig. 7. Effects caused by elliptic (transverse and longitudinal) oscillations

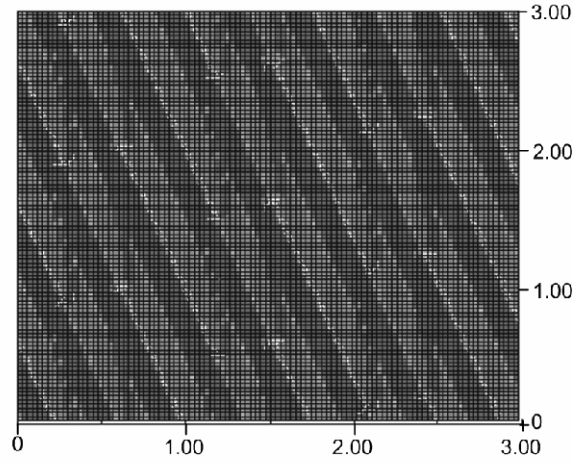

Fig. 8. Effects caused by elliptic oscillations (2D projection)

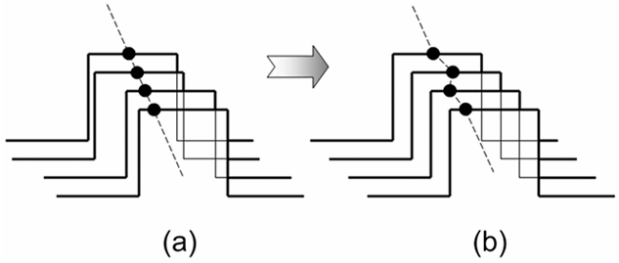

Fig. 9. Schematic diagram of correlation effect between two scanning lines: (a) – image before correlation; (b) – image after correlation

Let's suppose that the analyzed one dimensional surface oscillates harmonically only in the longitudinal direction. AFM measures the instantaneous height of this surface at equally spaced time moments t_i, $i = 0, 1, 2, ..., n$.

The geometric coordinate of the *i*-th scanned node at time moment t_i is $ih + \delta(t_i)$, where $\delta(t_i) = B\cos(\omega \cdot t_i + \varphi)$, B is the amplitude of longitudinal oscillations (Fig. 10(a)). Let the measured instantaneous heights at the geometric points $ih + \delta(t_i)$ be denoted as $I\left(ih + \delta(t_i)\right)$.

Then instantaneous heights of the surface at points ih, $i = 0, 1, 2, ..., n$, must be determined in order to perform the correlation procedure (Fig. 10 (b)).

Calculation of the height at any point *lh* can be performed as follows. At first we search for the two nearby points of *lh* (for example, $kh + \delta(t_k)$ and $(k+1)h + \delta(t_{k+1})$ (Fig. 10 (a), (b))). Then the instantaneous height at the point *lh is* calculated as (Fig. 10 (c)):

$$I\left(lh\right) = I\left(kh + \delta\left(t_k\right)\right) + \left(lh - kh + \delta(t_k)\right) \cdot \frac{I((k+1)h + \delta(t_{k+1})) - I(kh + \delta(t_k))}{\delta(t_{k+1}) - \delta(t_k) + h}. \quad (7)$$

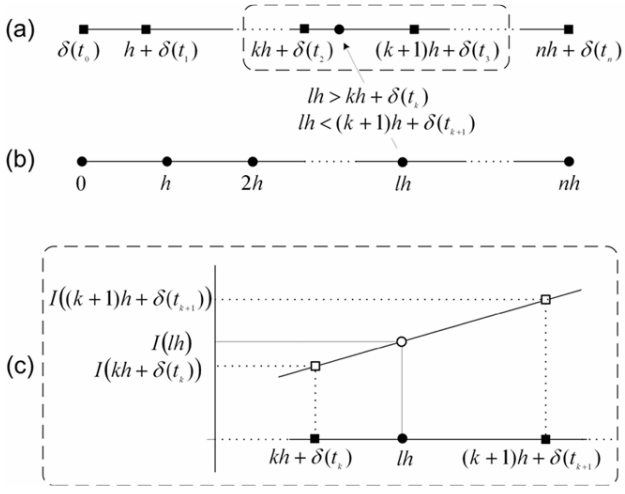

Fig. 10. Schematic graphical representation of the correlation procedure

It must be noticed that correlation process should be performed only in the regions where the surface gradient exceeds a predefined limit – there is no need to change the image where the surface gradient is small. The illustration of such case is presented in Fig. 11, where the analyzed one dimensional surface (Fig. 11 (a)) oscillates in both the transverse and longitudinal directions. Areas of relatively large gradient of the surface can be identified by the digital mask (Fig. 11 (d)). Finally, the reconstructed image is presented in Fig. 11 (e).

Analogously, correlation process can be performed for two dimensional images. A typical image used to illustrate the correlation effect between two scanning lines is presented in Fig. 12. Distorted image by elliptic oscillations is shown in Fig. 13. We use automatically generated digital mask to identify the regions of the image where the surface gradient exceeds a predefined limit (digital mask for Fig. 12 is presented in Fig. 14). Next, digital image is correlated mimicking the automatic manipulations with digital images performed by AFM. The correlation process is performed only in the area identified by the mask. Thus, local curvature of the grating lines can be clearly seen in the reconstructed image which is presented in Fig. 15.

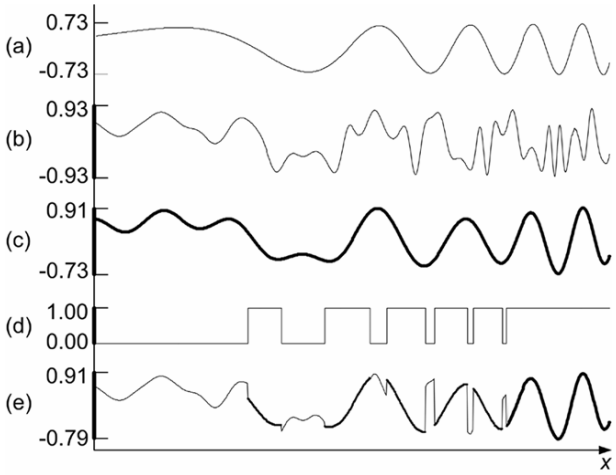

Fig. 11. One-dimensional example: (a) Original image; (b) Image distorted by elliptic oscillations; (c) Distorted image after correlation procedure; (d) Gradient mask of the image (a); (e) Reconstructed image using gradient mask

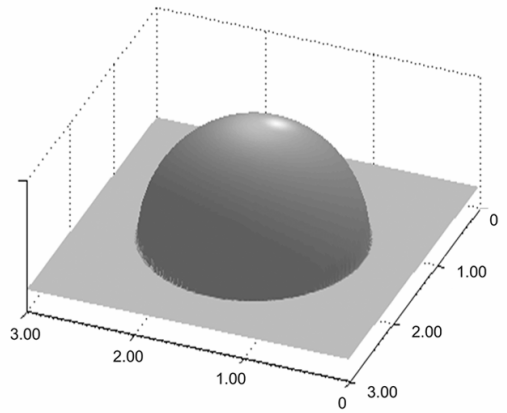

Fig. 12. Original image

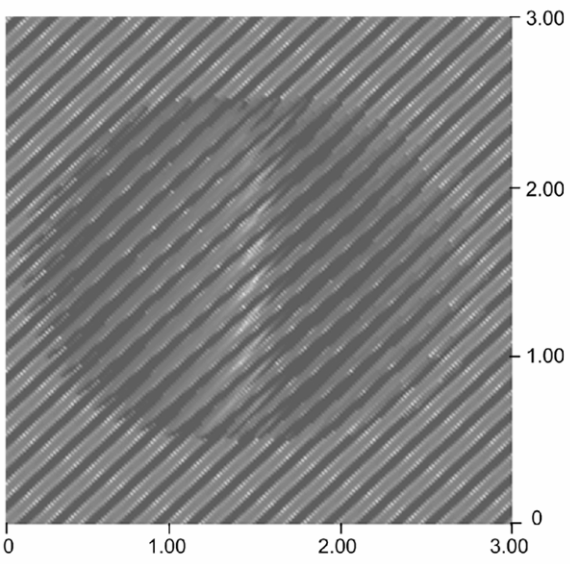

Fig. 13. Image distorted by elliptic oscillations

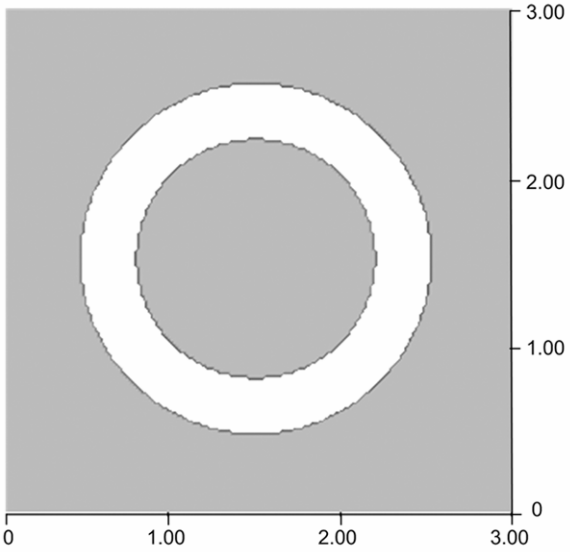

Fig. 14. Mask of the image represented in Fig. 12

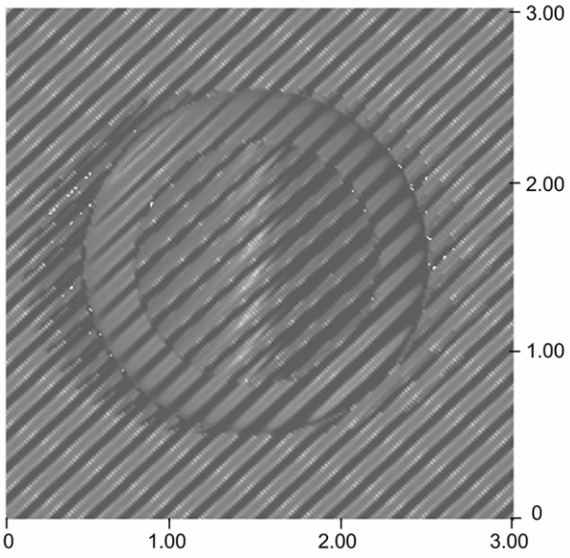

Fig. 15. Reconstructed image using mask

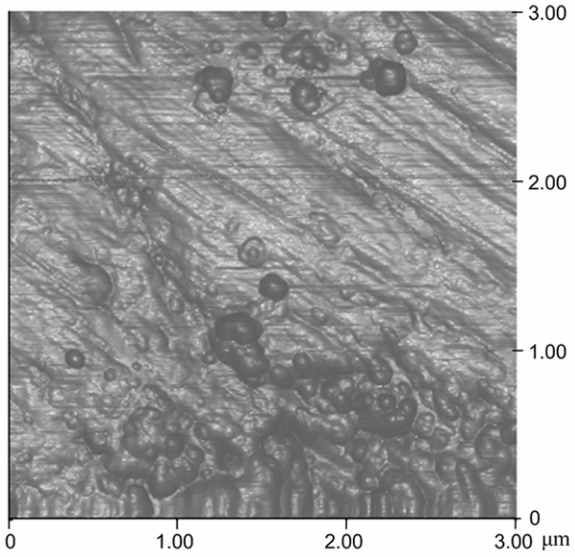

Fig. 16. Numerically reconstructed static surface

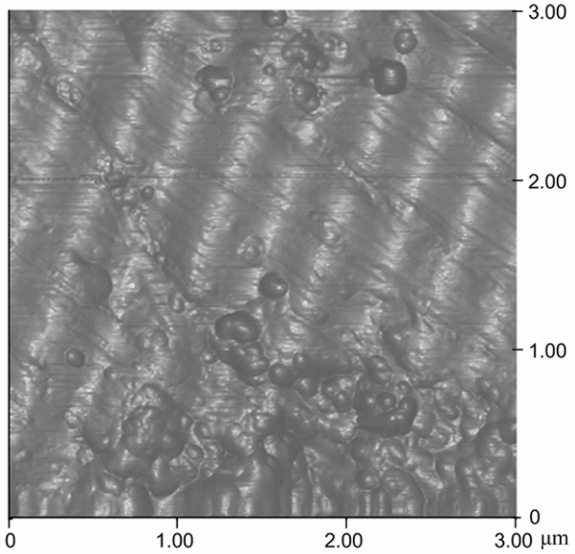

Fig. 17. Numerically reconstructed scanning process; transverse oscillations at $\omega = 9.4$ Hz

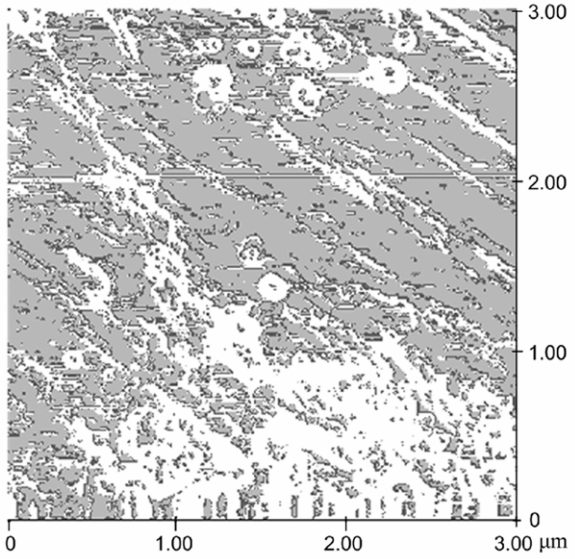

Fig. 18. Gradient mask, $\omega = 105$ Hz

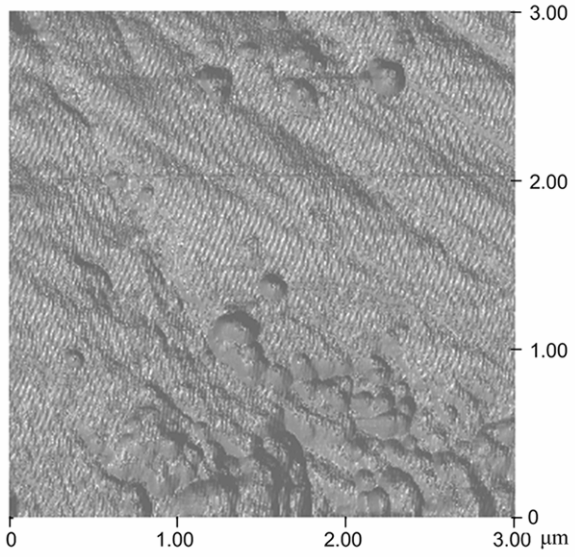

Fig. 19. Reconstructed image; elliptic oscillations, $\omega = 105$ Hz

The described method of image reconstruction is applied also for the static experimental image (Fig. 16). Scanning effects caused by transverse oscillations are illustrated in Fig. 17. The gradient mask of Fig. 16 is shown in Fig. 18. Finally, reconstructed image is presented in Fig. 19 where the density and local curvature of grating lines can be effectively used for identification of parameters of oscillation.

Concluding Remarks

A technique for AFM measurement of elliptic vibrations of piezoelectric ceramics is presented in this paper. Though the interpretable range of frequencies is rather limited, such measurements can be of a high value for testing properties of piezoelectric materials.

The observable grating caused by the periodic oscillation of the measured surface can be used for identification of the amplitude of vibrations. Non-dimensional amplitude of vibrations can be directly determined from 3D projections of the digital images. Calibration of the interpretable height then results into accurate determination of the nanoscale amplitudes.

References

[1] **Storck H., Wallaschek J.** Experimental investigations on modelling assumpltions in the stator / rotor contact of travelling wave ultrasonic motors. *Journal of Vibroengineering, Vol. 2, No. 4, 2000, Pages 77 – 83.*

[2] **Pons J. L., Rodríguez H., Seco F., Ceres R., Calderón L.** Modelling of piezoelectric transducers applied to piezoelectric motors: a comparative study and new perspective. *Sensors and Actuators A: Physical, Vol. 110, No.1-3, 2004, Pages 336-343.*

[3] **Roh Y., Kwon J.** Development of a new standing wave type ultrasonic linear motor. *Sensors and Actuators A: Physical, Vol. 112, No. 2-3, 2004, Pages 196-202.*

[4] **Santana-Gil A., Pelaiz-Barranco A., Rodriguez-Lopez L.** Low-cost and easy experiment to study the electromechanical resonance of piezoelectric ceramics. *Review of Scientific Instruments, Vol. 76, No. 1, 2005, Art. No. 013908.*

[5] **Muneishi T., Tomikawa Y.** Ultrasonic linear motor with two independent vibrations. *Japanese Journal of Applied Physics, Vol. 43, No. 9B, 2004, Pages 6728-6732.*

[6] **Eremkin V. V., Smotrakov V. G., Aleshin V. A., Tsikhotskii E. S.** Microstructure of porous piezoceramics for medical diagnostics. *Inorganic Materials, Vol. 40, No. 7, 2004, Pages 775-779.*

[7] **Liu M. C., Chen L. W.** Digital atomic force microscope Moire method. *Ultramicroscopy, Vol. 101, No. 2-4, 2004, Pages 173-181.*

[8] **Xie H. M., Asundi A., Boay C. G., Lu Y. G., Yu J., Zhong Z. W., Ngoi B. K. A.** High resolution AFM scanning Moiré method and its application to the micro-deformation in the BGA electronic package. *Microelectronics Reliability, Vol. 42, No. 8, 2002, Pages 1219-1227.*

[9] **Xie H. M., Boay C. G., Liu T., Lu Y. G., Yu J., Asundi A.** Phase-shifting moiré method with an atomic force microscope. *Applied Optics, Vol. 40, No. 34, 2001, Pages 6193-6198.*

[10] **Ragulskis M., Maskeliunas R.** Measurement of transverse vibrations of piezoelectric ceramics by atomic force microscopy. *Experimental Techniques, Vol. 30, No. 2, 2006, Pages 37-41.*